

# Demonstration of Computationally Efficient Vapor Injection Optimization Method for Spool Compressor



M. Mohsin Tanveer, Craig R. Bradshaw, Joe Orosz, and Greg Kemp

**Abstract** A heat pump is often considered a substitute for the conventional boiler due to its high efficiency. However, its performance is degraded when used in regions with extremely low outdoor temperatures. The refrigerant vapor injection technique is proven to improve the performance in refrigeration applications and it recently gained attention for heat pumping in cold climates. This article first develops a simplified approach to finding the equilibrium injection mass flow rate using a vapor compression cycle coupled with a mechanistic chamber model of a compressor. A novel spool compressor is then simulated with vapor injection for a wide range of operating conditions ( $-30^{\circ}\text{F}$  to  $35^{\circ}\text{F}$  evaporator temperature and  $110^{\circ}\text{F}$  condenser temperature). The effect of the injection port diameter and its angular location is also evaluated. The compressor simulation model is based on the mechanistic chamber modeling approach and is validated using experimentally collected data for different refrigerants, operating conditions and cooling capacities. The preliminary results indicate the existence of an optimal injection port diameter of 0.4 in. and port location between  $260^{\circ}$  and  $280^{\circ}$ .

**Keywords** Vapor injection · Heat pump · Compressor modeling

## Nomenclature

$\dot{m}_{leak,x}$	Mass flow rate through leakage path [ $\text{kg/s}$ ]
$A_{leak}$	Flow area of a leakage path [ $\text{m}^2$ ]
$\rho$	Density of the refrigerant [ $\text{kg/m}^3$ ]
$V$	Flow velocity of refrigerant [ $\text{m/s}$ ]
$tf_{tdc}$	Leakage through the top dead center [-]
$tf_t$	Leakage over the tip seal [-]
$tf_w$	Leakage through wrap-around gap [-]

---

M. M. Tanveer (✉) · C. R. Bradshaw  
Center for Integrated Building Systems, Oklahoma State University, Stillwater, OK 74078, USA  
e-mail: [mohsin.tanveer@okstate.edu](mailto:mohsin.tanveer@okstate.edu)

J. Orosz · G. Kemp  
Torad Engineering LLC, Cumming, GA 30040, USA

$tf_v$	Leakage over axial end of the vane [-]
$tf_f$	Leakage across axial end of face seal [-]
$tf_x$	Tuning factor xth leakage gap [-]
$V_{disp}$	Displacement volume [ $\text{in}^3$ ]
$T_{para}$	Parasitic torque [lbf-in]
$\theta_{inj,s,e}$	Starting or ending angle of injection port [deg]
$d_{inj}$	Injection port diameter [m]
$R_{stator}$	Stator radius [m]
$A_{leak,inj}$	Area of leakage path due to injection port [ $\text{m}^2$ ]
$\theta_{vane}$	Instantaneous angular location of vane [deg]
$\theta_{inj}$	Central angular location of injection port [deg]
$\eta_{o,is}$	Overall isentropic efficiency [-]
$P$	Compressor power [W]

## 1 Introduction

The refrigerant injection technique is a widely accepted method for enhancing the efficiency and reliability of heat pumps, especially in harsh weather conditions. The technique involves the introduction of a portion of refrigerant from the condenser outlet into the compression chamber, resulting in a reduced discharge temperature and a more efficient compression process [1]. There are three different refrigeration injection techniques, liquid injection, vapor injection, and two-phase injection [2]. This work focuses on the vapor injection technique in a spool compressor, which can be operated through an internal heat exchanger or a flash tank [3].

The internal heat exchanger technique involves extracting a small amount of refrigerant downstream of the condenser, which is then expanded to a specific intermediate pressure and used to cool the remaining refrigerant from the condenser. This extracted refrigerant is then injected into the compressor as a saturated vapor. On the other hand, the flash tank-based vapor injection technique involves expanding the entire refrigerant downstream of the condenser to a two-phase state, with the vapor being injected into the compressor and the liquid entering another expansion valve. Several studies have shown that flash tank systems have better thermodynamic potential compared to other vapor injection methods [4]. As a result, the flash tank-based vapor injection technique is adopted in this study.

The optimization of various parameters is crucial for the effective implementation of vapor injection. Unlike conventional compressor operation where the efficiency depends on the refrigerant state at the source and sink, the efficiency of a vapor injection-based compressor also depends on the injection state. While the injection pressure is often assumed to be the geometric mean of the suction and discharge pressure [5], this study suggests that the best injection pressure depends on several factors such as the injection port diameter and location.

In this article, a physics-based mechanism is developed to optimize the injection pressure, injection port size, and location. The optimization method is used to find the optimum injection port for R1234yf, and a mechanistic chamber model is used to predict the performance of the vapor injection-based spool compressor.

## 2 Mechanistic Chamber Model

The mechanistic chamber model is 0D model that simulates the compressor performance by employing the mass and energy balance principles to discrete chambers or control volumes within a specific type of compressor. The model takes into account the instantaneous chamber volume change, mass flows between different chambers, movement of mechanical elements, heat transfer and refrigerant properties. A comprehensive review of the mechanistic chamber model is presented in [6] while a tailored version of the model specifically for spool compressors is discussed in [7].

### 2.1 Model Validation

The mechanistic chamber model necessitates the tuning of parameters that are specific to a compressor design and dependent on the manufacturing tolerances. Such parameters encompass the leakage paths and friction coefficients. In the case of the spool compressor, leakage tuning factors are introduced in the mass flow equation as,

$$\dot{m}_{leak,x} = t f_x \cdot A_{leak} \cdot \rho \cdot V, \quad (1)$$

which modifies the calculated mass flow rate from the isentropic nozzle flow model to align with the experimentally determined mass flow rate. A trial-and-error approach is employed to fine-tune these factors and it was observed that there is a correlation between the leakage flow rate and the compressor pressure ratio. Thus, the final form of the leakage tuning factors is expressed as a function of the pressure ratio for multiple leakage paths that exist. The calibration equation for each of the leakage paths is listed below.

$$t f_{dc} = 0.0588 P R + 0.084 \quad (2)$$

$$t f_t = 0.1096 P R + 1.7245 \quad (3)$$

$$t f_w = 0.0114 P R + 0.0792 \quad (4)$$

$$t f_v = 0.0012 P R + 0.0108 \quad (5)$$

$$t f_f = 0.1067 P R + 0.2453 \quad (6)$$

In order to reconcile the compressor power and isentropic efficiency with the experimental data, and additional four distinct parameters are adjusted for model tuning. These parameters are as follows:

- $\mu_{seal}$ : Dry friction coefficient between the seal face and the rotating end plate
- $\mu_{seal,bevel}$ : Dry friction coefficient between the bevel surface and the cylinder
- $\mu_{gate}$ : dry friction coefficient between vane and rotor
- $filmfraction$ : tuning factor for frictional models

These parameters include friction coefficients between various rotating components of the spool compressor and a tuning factor that adjusts all frictional losses. A value of 1.2, 0.2, 0.1, and 0.04 for  $\mu_{seal}$ ,  $\mu_{seal,bevel}$ ,  $\mu_{gate}$ , and  $filmfraction$ , respectively, was found to provide good agreement with experimental results.

Additionally, another parameter, parasitic torque  $T_{para}$ , is introduced which accounts for losses that are not included in the model. These losses may include valve and manifold losses, contributing up to 5–6% of the total compressor power. The contribution of this parasitic loss can vary between 2 and 10% of the total power depending on various conditions. Based on the experimental data, a piece-wise equation has been developed to calculate the parasitic torque for various displacement volumes of the compressor. This equation can be represented as follows,

$$\begin{cases} T_{para} = (0.00459 * V_{disp} - 0.00291) * 160 & 1 < V_{disp} < 50, \\ T_{para} = (0.01389 * V_{disp} - 0.46713) * 160 & V_{disp} > 50, \end{cases}$$

where,  $V_{disp}$  is the maximum displacement volume of a compression chamber in  $in^3$ .

Figure 1 compares the results from the calibrated model with the experimental results and suggests that the model can predict the mass flow rate, volumetric efficiency and power within Mean Absolute Error (MAE) of 1.9%, 2.9%, 2.6% and isentropic efficiency 2.04%, respectively. This validates that the model is sufficiently accurate in its base formulation and will need to be updated to include vapor injection.

### 3 Model Updates to Include Vapor Injection in Mechanistic Chamber Model

To incorporate the simulation of vapor injection in the spool compressor, updates were made to the existing, validated, mechanistic chamber model. A sub-model was added to the overall model to calculate the injection mass flow rate into the different chambers of the spool compressor, based on the pressure difference across the port and the port's angular location. At any given moment, there are two or three different chambers, which are dependent on the angular position of the vane. The detailed formulation of these chambers and their movement is described in [7]. In the vapor injection sub-model, the model first identifies the chamber that is interacting with the injection port (Fig. 2), and then calculates the mass flow rate across the injection

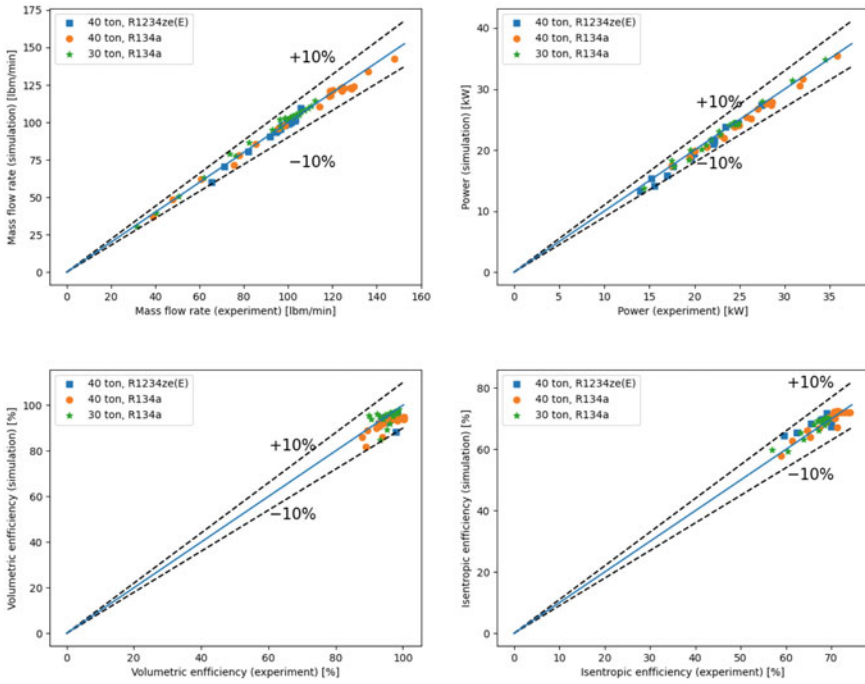


**Fig. 1** Spoolcompressor predicted performance compared to the experimental results for two compressor sizes and two refrigerants

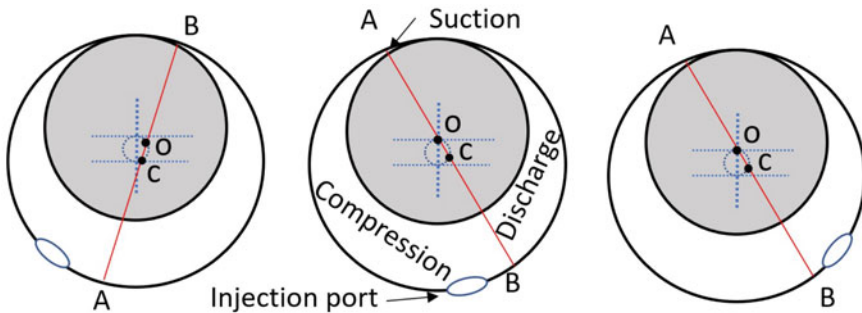


**Fig. 2** Three different injection port locations and their interaction with suction, compression and discharge chamber

port using the isentropic nozzle flow model. This calculated injection mass flow rate is used in the mass and energy balance equations to calculate the refrigerant state at the next integration step [6].

The addition of an injection port to the compressor stator introduces another leakage path as the vane travels across the injection port. To account for this, a

leakage model has been added to calculate the mass flow rate from the high-pressure chamber to the low-pressure chamber. In the optimization model, the model iterates over the injection angle, which represents the central position of the port. Using,

$$\theta_{inj,s,e} = \theta_{inj} \pm \frac{d_{inj}}{2R_{stator}}, \tag{7}$$

the leakage model calculates the starting and ending angle of the injection port using the port diameter and stator radius, where  $\theta_{inj,s,e}$  and  $d_{inj}$  represent the starting and ending angle of the injection port and the injection port diameter, respectively, and  $R_{stator}$  is the stator radius. The leakage area is modeled to vary in a sinusoidal pattern between the starting and ending angles of the injection port. This variation is calculated using,

$$A_{leak,inj} = (A_{max} - A_{min})/2(\sin(2(\theta_{vane} - \theta_{inj}) + \pi/2) + 1) + A_{min}, \tag{8}$$

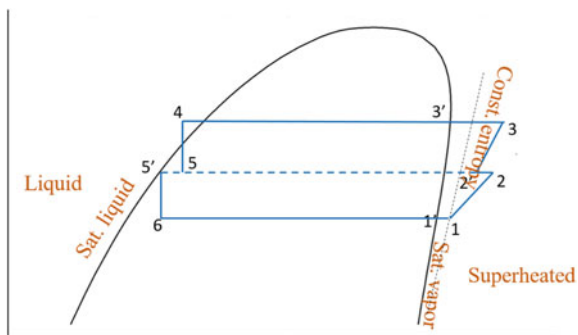
where  $A_{max}$  equals the half of the cross-sectional area of the port,  $A_{min}$  is set to zero, and  $\theta_{vane}$  represents the instantaneous angular position of the vane in the integration process. The location of the vane relative to the injection port is determined and, when the vane passes over the injection port, the model calculates which two of the three chambers are present and calculates the instantaneous mass flow rate from the high-pressure chamber to the low-pressure chamber using the isentropic nozzle flow model. The leakage mass flow rate is then incorporated into the mass and energy conservation equations to predict the next state of the refrigerant in each chamber.

The isentropic efficiency of the compressor is calculated according to the ASHRAE standards 23 [8] and can be represented as,

$$\eta_{o,is} = \frac{\dot{m}_1(h_{2s} - h_1) + \dot{m}_3(h_{3s} - h_{2'})}{P}, \tag{9}$$

where  $\dot{m}_1$  is the suction mass flow rate,  $\dot{m}_3$  is the discharge mass flow rate and refrigerant state points are shown in Fig. 3. The compressor power is calculated as,

**Fig. 3** P-h plot of flash tank based simple vapor compression cycle



$$P = \dot{m}_1(h_3 - h_1) + \dot{m}_2(h_3 - h_2), \tag{10}$$

where,  $m_2$  is the injection mass flow rate.

### 4 Optimization Model

A schematic of the optimization algorithm is shown in Fig. 4. The algorithm starts with the assumptions of port diameter, injection angle, and injection pressure. The guess port diameter is linked with the discharge port size to ensure the model is suitable for different compressor sizes and falls between 1/3 to 2/3 of the discharge port diameter. The injection angle is varied between 260 and 280°, as preliminary analysis shows a rapid drop in volumetric efficiency below 260° and discharge ports lie a little over 280°. The two extremes of injection pressure are 150 kPa above and below the suction and discharge pressure, respectively. Using these ranges, the mechanistic chamber model predicts compressor performance for different combinations of these parameters.

The mechanistic chamber model predicts the injection mass flow rate based on the pressure difference between injection pressure and chamber pressure by using an isentropic nozzle flow model. This predicted mass flow rate could be more or less than the mass flow rate available from the flash tank. A complete iterative solution of the Vapor Compression Cycle (VCC) is required for an accurate prediction of mass flow rate, but this leads to high computational time. To reduce computation time, a simplified method is employed that finds the equilibrium injection pressure. The process starts by calculating the injection mass flow rate and discharge mass

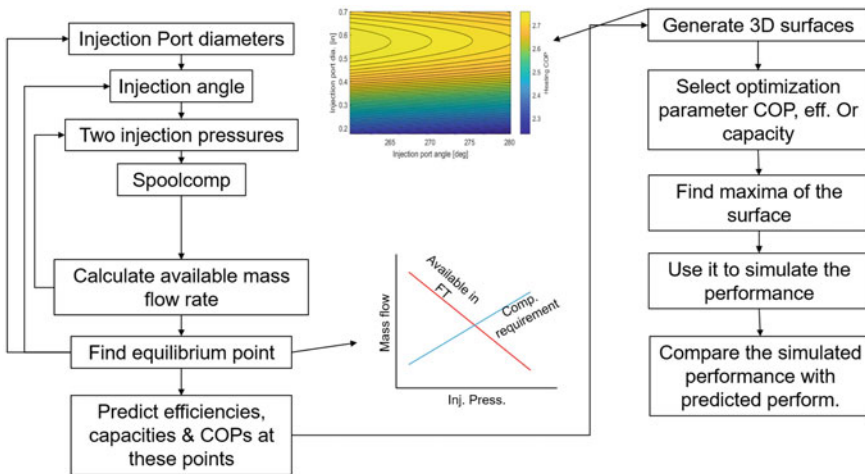


Fig. 4 Flow chart for the optimization model

flow rate using the mechanistic chamber model at the two extreme injection pressure values. The quality of the refrigerant at these pressures is calculated using the cycle analysis shown in Fig. 3. The quality and discharge flow rate are used to calculate the injection mass flow rate available in the flash tank for each injection pressure. The equilibrium pressure is found at the intersection of the calculated injection mass flow rate and the cycle analysis. The compressor performance parameters are predicted at this point using a linear curve fit between the two extreme results obtained from the mechanistic chamber model. This process is repeated for all port diameter and angle combinations and a 3-D surface plot and curve fit equations are developed for performance parameters. The optimum port diameter and angle are found and used to predict performance.

## 5 Results and Discussion

In this study, a novel optimization model is presented to determine the combination of vapor injection port diameter, port angle, and pressure that maximizes the heating coefficient of performance (COP) of a spool compressor. The analysis is conducted for 132 in<sup>3</sup> displacement volume and R1234yf refrigerant. The two operating conditions ( $-30^{\circ}\text{F}/110^{\circ}\text{F}$  and  $35^{\circ}\text{F}/110^{\circ}\text{F}$ ) were chosen for preliminary analysis which represent two extremes of conditions for heat pump application. The model leverages a mechanistic chamber approach to simulate the compressor performance. The mechanistic chamber model is validated for different compressor sizes, refrigerants and operating ranges. A simplified modeling technique is developed to ensure that the injection mass flow rate, predicted by the mechanistic chamber model, is in balance with the vapor compression cycle.

Figure 5 presents the impact of injection port diameter and angle on the heating COP, displayed through contour plots for two different operating conditions. The results indicate that for this particular compressor, the optimum injection diameter is

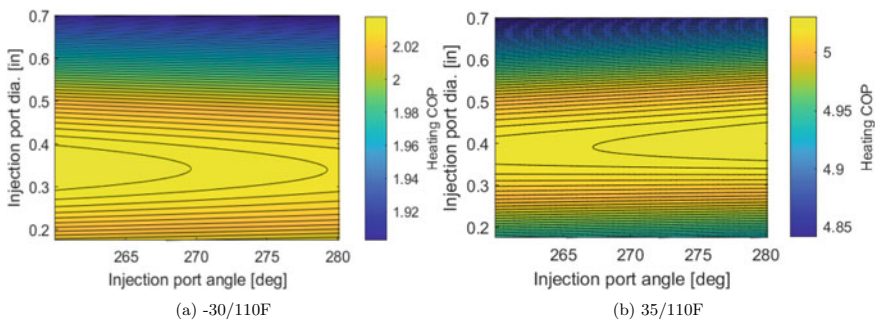


**Fig. 5** Contour plots representing the change in the heating COP w.r.t injection port diameter and angle



around 0.4 in, yielding a heating COP variation of up to 0.2 for various injection port diameters. Additionally, the best heating COP is independent of the injection port angle within the optimized range of 260–280°. This range was selected to avoid a reduction in volumetric efficiency, which occurs when the injection port and suction port intersect, causing backflow. The developed methodology can be used to explore the optimum injection port specifications for a wide range of compressor sizes, refrigerants and operating conditions. Also, the results from this study will be used to develop a spool compressor prototype with vapor injection.

## 6 Conclusion

A simplified method is developed that calculates the equilibrium vapor injection mass flow rate of VCC in a very short time and iterates over injection port diameter, port angle and injection pressure to find the optimum combination of parameters to achieve the best heating COP. A mechanistic chamber model based spool compressor model is validated with the experimental results and is used for performance evaluation. The preliminary results suggest that the 0.4 in injection port diameter is desirable to achieve the best performance with the vapor injection cycle. The demonstrated model will be used to find the optimum injection port design for future low-GWP refrigerants and heat pump applications.

## References

1. D. Kim et al., Performance comparison among two-phase, liquid, and vapor injection heat pumps with a scroll compressor using R410A, in: *Applied Thermal Engineering* 137. Sept 2017 (2018), pp. 193–202. ISSN: 13594311. <https://doi.org/10.1016/j.applthermaleng.2018.03.086>. <https://doi.org/10.1016/j.applthermaleng.2018.03.086>
2. A. Khan, C.R. Bradshaw, Quantitative comparison of the performance of vapor compression cycles with various means of compressor flooding. 2739 (2022)
3. S. Jain et al., Vapor injection in scroll compressors. *Int. Compressor Eng. Cof.* 1642 (2004). ISBN: 2173337734. <https://docs.lib.purdue.edu/icec>
4. M.G. Yuan, Z.H. Xia, Experimental study of a heat pump system with flashtank coupled with scroll compressor. *Energy Buildings* 40(5), 697–701 (2008). ISSN: 03787788. <https://doi.org/10.1016/J.ENBUILD.2007.05.003>
5. A. Redón et al., Analysis and optimization of subcritical two-stage vapor injection heat pump systems. *Appl. Energy* 124, 231–240 (2014). ISSN: 03062619. <https://doi.org/10.1016/j.apenergy.2014.02.066>
6. M. Mohsin Tanveer et al., Mechanistic chamber models: a review of geometry, mass flow, valve, and heat transfer sub-models. *Int. J. Refrig.* 142(June 2022), 111–126. ISSN: 01407007. <https://doi.org/10.1016/J.IJREFRIG.2022.06.016>
7. C.R. Bradshaw, E.A. Groll, A comprehensive model of a novel rotating spool compressor. *Int. J. Refrig.* 36(7) (Nov. 2013), 1974–1981. ISSN: 0140-7007. <https://doi.org/10.1016/J.IJREFRIG.2013.07.004>
8. ANSI/ASHRAE, Methods for performance testing positive displacement refrigerant compressors and compressor units, in *ANSI/ASHRAE Standard* 23-2022 vol. 23(2) (2022)